

Evidence for charged critical behavior in the pyrochlore superconductor RbOs_2O_6

T. Schneider¹, R. Khasanov^{1,2,3}, and H. Keller¹

⁽¹⁾ *Physik-Institut der Universität Zürich,
Winterthurerstrasse 190,
CH-8057 Zürich, Switzerland*

⁽²⁾ *Laboratory for Neutron Scattering, ETH Zürich
and PSI Villigen,*

CH-5232 Villigen PSI, Switzerland

⁽³⁾ *DPMC, Université de Genève, 24 Quai
Ernest-Ansermet,*

CH-1211 Genève 4, Switzerland

We analyze magnetic penetration depth (λ) data of the recently discovered superconducting pyrochlore oxide RbOs_2O_6 . Our results strongly suggest that in RbOs_2O_6 charged critical fluctuations dominate the temperature dependence of λ near T_c . This is in contrast to the mean-field behavior observed in conventional superconductors and the uncharged critical behavior found in nearly optimally doped cuprate superconductors. However, this finding agrees with the theoretical predictions for charged criticality and the charged criticality observed in underdoped $\text{YBa}_2\text{Cu}_3\text{O}_{6.59}$.

Transition metal (TM) oxides are of considerable interest because their properties range from metal-insulator transitions to colossal magnetoresistance and superconductivity. TM oxide compounds with the pyrochlore structure have long been studied and have found many applications [1], but it is not until recently that superconductivity was discovered in one such a material, namely $\text{Cd}_2\text{Re}_2\text{O}_7$ at $T_c \approx 1$ K [2–4]. Subsequently, superconductivity was also discovered in the pyrochlore oxides KOs_2O_6 ($T_c \approx 9.6$ K) [5], RbOs_2O_6 with ($T_c \approx 6.3$ K) [6] and CsOs_2O_6 with ($T_c \approx 3.3$ K) [7]. Although the T_c 's are rather low the discovery of superconductivity in the pyrochlore oxides opens research in this area to a new class of materials and raises, of course, the question of the underlying mechanism. Based on a Cd and Re NMR/NQR study Vyaselev *et al.* [8] concluded that $\text{Cd}_2\text{Re}_2\text{O}_7$ behaves as a weak-coupling BCS superconductor with a nearly isotropic gap, in agreement with specific heat measurements [9]. On the other hand, Koda *et al.* [10] interpreted their penetration depth measurements on KOs_2O_6 in terms of unconventional superconductivity, while the recent specific heat [11], magnetization, muon-spin-rotation (μSR) measurements of the magnetic penetration depth [12,13], and the pressure effect measurements [12] on RbOs_2O_6 reveal consistent evidence for mean-field behavior, except close to T_c , where thermal fluctuations are expected to occur. Hence, a careful study of the thermodynamic properties of these materials close to T_c should allow to discriminate between mean-field, charged and uncharged critical behavior.

In this work, we focus on RbOs_2O_6 and analyze the extended measurements of the temperature dependence of the magnetic penetration depth λ [13]. Our results strongly suggest that RbOs_2O_6 falls in the universality class of charged superconductors because charged critical fluctuations are found to dominate the temperature dependence of λ near T_c . It differs from the mean-field behavior observed in conventional superconductors and the uncharged critical behavior found in nearly optimally doped cuprate superconductors [14–18], but agrees with the theoretical predictions for charged criticality [19–23] and the charged critical behavior observed in underdoped $\text{YBa}_2\text{Cu}_3\text{O}_{6.59}$ [24].

As long as the effective dimensionless charge $\tilde{e} = \xi/\lambda = 1/\kappa$ [14] is small, where κ is the Ginzburg-Landau parameter, the crossover upon approaching T_c is initially to the critical regime of a weakly charged superfluid where the fluctuations of the order parameter are essentially those of an uncharged superfluid [14–18]. However, superconductors with rather low T_c 's and far away from any quantum critical point are expected to exhibit mean-field ground state properties. In this case the Ginzburg-Landau parameter scales with the specific heat coefficient γ as $\kappa \propto \lambda^2(0) \sqrt{\gamma T_c}$ [25]. Thus, the superconducting pyrochlores, with rather low T_c 's and moderate γ and $\lambda(0)$ values appear to open up a window onto the charged critical regime.

Here we concentrate on the analysis of the magnetic penetration depth data derived from Meissner fraction measurements [13]. These data are in excellent agreement with the μSR measurements [12,13] and sufficiently dense to explore the critical behavior near T_c . As required for the determination of the magnetic penetration depth λ from the Meissner fraction measurements the sample was ground in order to obtain small grains [13]. Assuming spherical grains of radius R their size distribution was deduced from SEM (scanning electron microscope) photographs. The resulting particle size distribution $N(R)$ is shown in Fig.1.

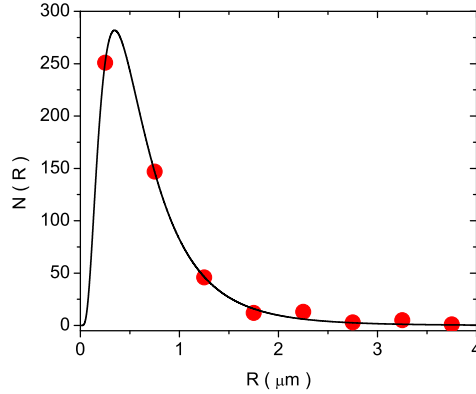


FIG. 1. Grain size distribution $N(R)$ of our RbOs_2O_6 sample taken from Khasanov *et al.* [13]. The solid line is a fit to the log-normal distribution [26].

The data for the temperature dependence of the penetration depth was deduced by Khasanov *et al.* [13] from the measured Meissner fraction $f(T)$ by using the Shoenberg formula [27] modified for the known grain size distribution [28],

$$f(T) = \int_0^\infty \left(1 - \frac{3\lambda(T)}{R} \coth\left(\frac{R}{\lambda(T)}\right) + \frac{3\lambda^3(T)}{R^2} \right) / \int_0^\infty g(R) dR, \quad (1)$$

where $g(R) = N(R) R^3$ is the fraction distribution.

In Fig.2 we depicted the resulting data in terms of $(d \ln \lambda / dT)^{-1}$ vs. T . In a homogeneous and infinite system λ diverges as

$$\lambda = \lambda_0 |t|^{-\tilde{\nu}}, \quad t = T/T_c - 1, \quad (2)$$

where $\tilde{\nu} = 1/2$ for a conventional mean-field superconductor, $\tilde{\nu} = 1/3$ when uncharged thermal fluctuations dominate [14–17] and $\tilde{\nu} = 2/3$ when the charge of the pairs is relevant [19–23]. Furthermore, when charged fluctuations dominate the penetration depth and the correlation length are near T_c related by [19–23]

$$\lambda = \kappa \xi, \quad (3)$$

contrary to the uncharged case, where $\lambda \propto \sqrt{\xi}$. κ denotes the Ginzburg-Landau parameter. In the plot $(d \ln \lambda / dT)^{-1}$ vs. T shown in Fig.2 critical behavior is then uncovered if the data collapse close to T_c on a line with slope $1/\tilde{\nu}$. Interestingly enough the data points clearly to charged critical behavior (solid line with $1/\tilde{\nu} \simeq 3/2$), limited by a finite size effect due to the finite extent of the grains and/or inhomogeneities within the grains. Indeed, although charged criticality is attained there is no sharp transition, because $\xi = \lambda/\kappa$ cannot grow beyond the limiting length L and with that λ does not diverge at T_c .

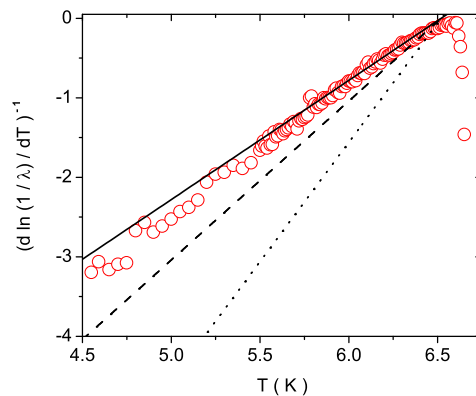


FIG. 2. $(d \ln \lambda / dT)^{-1}$ with λ in μm versus T for RbOs_2O_6 derived from the data of Khasanov *et al.* [13]. The solid line with slope $1/\tilde{\nu} \simeq 3/2$ corresponds according to Eq. (2) to charged criticality with $T_c = 6.52$ K, while the dashed line indicates mean-field behavior ($1/\tilde{\nu} \simeq 2$) and the dotted one 3D-XY critical behavior ($1/\tilde{\nu} \simeq 3$).

To explore the evidence for charged critical behavior and the nature of the finite size effect further, we displayed in Fig. 3 $1/\lambda_{ab}$ and $d(1/\lambda_{ab})/dT$ vs. T . The solid line is Eq. (2) with $T_c = 6.52$ K, $\lambda_0 = 0.212$ μm and $\tilde{\nu} = 2/3$, appropriate for charged criticality, and the dashed one its derivative. Approaching T_c of the fictitious homogeneous and infinite system the data reveals clearly a crossover to charged critical behavior, while the tail in $1/\lambda$ vs. T around T_c points to a finite size effect, because $d\lambda/dT$ does not diverge at T_c but exhibits at $T_p \simeq 6.48$ K an extremum. For this reason $1/\lambda(T)$ possesses an inflection point at T_p and the correlation length attains the limiting length L .

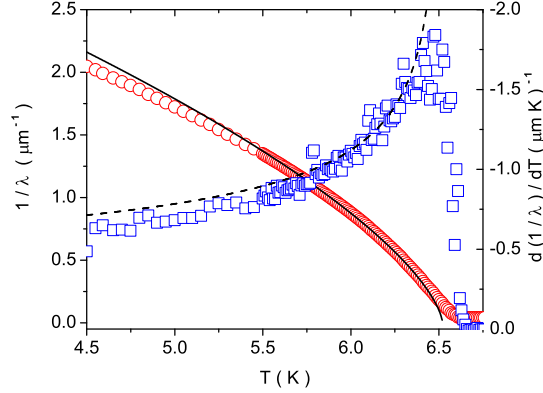


FIG. 3. $1/\lambda$ and $d(1/\lambda)/dT$ vs. T for RbOs_2O_6 derived from the data of Khasanov *et al.* [13]. The solid line is Eq.2 with $T_c = 6.52$ K, $\lambda_0 = 0.212$ μm and $\tilde{\nu} = 2/3$, corresponding to the charged case, while the dashed line is the derivative.

In this case the penetration depth adopts the finite size scaling form [29,30]

$$\lambda(T) = \lambda_0 |t|^{-\tilde{\nu}} g(y), \quad y = \text{sign}(t) \left| \frac{t}{t_p} \right|, \quad (4)$$

with $\tilde{\nu} \simeq 2/3$ and $\xi(T_p) = \xi_0 |t_p|^{-\tilde{\nu}} = L$. For t small and $L \rightarrow \infty$ the scaling variable tends to $y \rightarrow \pm\infty$ where $g(y \rightarrow -\infty) = 1$ and $g(y \rightarrow +\infty) = 0$, while for $t = 0$ and $L \neq 0$, $g(y \rightarrow 0) = g_0 |y|^{2/3} = g_0 |t/t_p|^{2/3}$. In this limit we obtain

$$\frac{\lambda(T_c, L)}{\lambda_0} = g_0 \frac{L}{\xi_0}. \quad (5)$$

In Fig. 4 we displayed the finite size scaling function $g(y)$ deduced from the measured data and the parameters emerging from the fits shown in Fig.3. The solid line indicates the asymptotic behavior $g(y \rightarrow 0) = g_0 |y|^{2/3}$ with $g_0 = 0.92$. The upper branch corresponding to $T < T_c$ tends to $g(|y| \rightarrow \infty) = 1$, while the lower one referring to $T > T_c$ approaches $g(|y| \rightarrow \infty) = 0$. Consequently, the absence of a sharp transition (see Figs. 2 and 3), is fully consistent with a finite size effect arising from a limiting length L , attributable to the finite extent of the grains and/or inhomogeneities within the grains. To disentangle these options we invoke Eq.(5) yielding with $\lambda(T_c, L) \simeq 6.45$ μm , $\lambda_0 \approx 0.212$ μm and $g_0 = 0.92$, $L/\xi_0 \approx 33$. An estimate of ξ_0 can be derived from the magnetic field dependence of the maximum of the specific heat coefficient [32]. As a remnant of the zero-field singularity, there is for fixed field strength a peak adopting its maximum at $T_p(H)$ which is located below T_c . $T_p(H)$ is given by $(1 - T_p(H)/T_c)^{4/3} = (aH\xi_0^2)/\Phi_0$, where $a \simeq 3.12$. From the specific heat data of Brühwiler *et al.* [11] we derive $\xi_0 \approx 0.008$ μm . Accordingly, $L \approx 33\xi_0 \approx 0.26$ μm . On the other hand, a glance to Fig.1 shows that the grain size distribution of the RbOs_2O_6 sample exhibits a maximum at ≈ 0.69 μm and decreases steeply for smaller grains. Hence, the smeared transition is not attributable to the finite extent of the grains but most likely due to inhomogeneities within the grains.

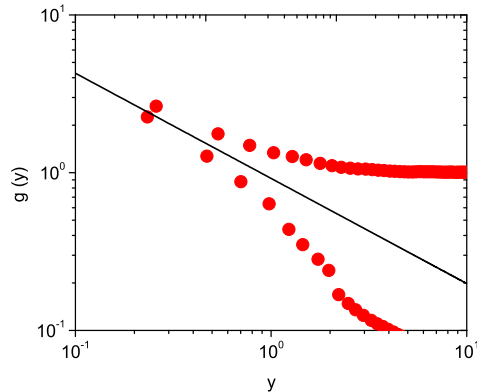


FIG. 4. Finite size scaling function $g(y)$ deduced from the measured data of Khasanov *et al.* [13] with $T_c = 6.52$ K, $T_p \simeq 6.48$ K, $\lambda_0 = 0.212$ μm and $\tilde{\nu} = 2/3$. The solid line indicates the asymptotic behavior $g(y \rightarrow 0) = g_0 |y|^\nu$ with $g_0 = 0.92$.

In summary, we have presented an extended analysis of penetration depth data for RbOs_2O_6 near T_c providing consistent evidence for charged critical behavior of the superconductor to normal state transition in type II superconductors ($\kappa_0 > 1/\sqrt{2}$). The crossover upon approaching T_c is thus to the charged critical regime, while in nearly optimally doped cuprates it is to the critical regime of a weakly charged superfluid where the fluctuations of the order parameter are essentially those of an uncharged superfluid. However, there is the inhomogeneity induced finite size effect which renders the asymptotic critical regime difficult to attain [31–33]. Nevertheless, our analysis of the penetration depth data of RbOs_2O_6 provides remarkable consistency for critical fluctuations, consistent with the charged universality class, limited close to T_c of the fictitious infinite and homogeneous counterpart by a finite size effect predominantly due to inhomogeneities within the grains. Accordingly our analysis strongly suggests that RbOs_2O_6 is not a conventional mean-field superconductor because charged critical fluctuations dominate the temperature dependence of the penetration depth near T_c . These fluctuations should also affect the specific heat [34] and the magnetic properties. However, more extended measurements near criticality are needed to uncover this behavior.

ACKNOWLEDGMENTS

The authors are grateful to B. Batlogg, M. Brühwiler, D. Di Castro and A. Sudbø for useful comments and suggestions on the subject matter. This work was partially supported by the Swiss National Science Foundation and the NCCR program *Materials with Novel Electronic Properties* (MaNEP) sponsored by the Swiss National Science Foundation.

-
- [1] M. A. Subramanian, G. Aravamudan, and G. V. S. Rao, *Prog. Solid St. Chem.* **15**, 55 (1983).
 - [2] M. Hanawa, Y. Muraoka, T. Tayama, T. Sakakibara, J. Yamaura, and Z. Hiroi, *Phys. Rev. Lett.* **87**, 187001 (2001).
 - [3] H. Sakai, K. Yoshimura, H. Ohno, H. Kato, S. Kambe, R. E. Walstedt, T. D. Matsuda, Y. Haga, and Y. Onuki, *J. Phys.: Condens. Matter* **13**, L785 (2001).
 - [4] R. Jin, J. He, S. McCall, C. S. Alexander, F. Drymiotis, and D. Mandrus, *Phys. Rev. B* **64**, 180503 (2001).
 - [5] S. Yonezawa, Y. Muraoka, Y. Matsushita and Z. Hiroi, *J. Phys.: Condens. Matter* **16**, L9 (2004).
 - [6] S. Yonezawa, Y. Muraoka, Y. Matsushita and Z. Hiroi, *J. Phys. Soc. Japan* **73**, 819 (2004).
 - [7] S. Yonezawa, Y. Muraoka and Z. Hiroi, *cond-mat/0404220*.
 - [8] O. Vyaselev, K. Kobayashi, K. Arai, J. Yamazaki, K. Kodama, M. Takigawa, M. Hanawa, and Z. Hiroi, *J. Phys. Chem. Solids* **63**, 1031 (2002).
 - [9] Z. Hiroi and M. Hanawa, *J. Phys. Chem. Solids* **63**, 1021 (2002).
 - [10] A. Koda, W. Higemoto, K. Ohishi, S. R. Saha, R. Kadono, S. Yonezawa, Y. Muraoka, and Z. Hiroi, *cond-mat/0402400*.
 - [11] M. Brühwiler, S.M. Kazakov, N.D. Zhigadlo, J. Karpinski, and B. Batlogg, *Phys. Rev. B* **70**, 020503 (2004).

- [12] R. Khasanov, D. G. Eshchenko, J. Karpinski, S. M. Kazakov, N. D. Zhigadlo, R. Brütsch, D. Gavillet, and H. Keller, cond-mat 0404542.
- [13] R. Khasanov, D. G. Eshchenko, D. Di Castro, A. Shengelaya, F. La Mattina, A. Maisuradze, C. Baines, H. Luetkens, J. Karpinski, S. M. Kazakov, and H. Keller, unpublished.
- [14] D. S. Fisher, M. P. A. Fisher and D. A. Huse, Phys. Rev. B **43**, 130 (1991).
- [15] T. Schneider and D. Ariosa, Z. Phys. B **89**, 267 (1992).
- [16] T. Schneider and H. Keller, Int. J. Mod. Phys. B **8**, 487 (1993).
- [17] T. Schneider and J. M. Singer, *Phase Transition Approach To High Temperature Superconductivity*, (Imperial College Press, London, 2000).
- [18] T. Schneider, in *The Physics of Superconductors*, edited by K. Bennemann and J. B. Ketterson (Springer, Berlin 2004) p. 111.
- [19] I. F. Herbut and Z. Tesanovic, Phys. Rev. Lett. **76**, 4588 (1996).
- [20] I. F. Herbut, J. Phys. A **30**, 423 (1997).
- [21] P. Olsson and S. Teitel, Phys. Rev. Lett., **80**, 1964 (1998).
- [22] J. Hove and A. Sudbø, Phys. Rev. Lett., **84**, 3426 (2000).
- [23] S. Mo, J. Hove, A. Sudbø, Phys. Rev. B **65**, 104501 (2002).
- [24] T. Schneider, R. Khasanov, K. Conder, E. Pomjakushina, R. Brütsch, and H. Keller, cond-mat/0406691.
- [25] P. G. de Gennes, *Superconductivity of Metals and Alloys*, (Benjamin, New York 1966).
- [26] J. Kiefer and J.B. Wagner, J. Electrochem. Soc. **135**, 198 (1988).
- [27] D. Shoenberg, Proc. R. Soc. Lond. **A 175**, 49 (1940).
- [28] A. Porch *et al.*, Phycica C **214**, 350 (1993).
- [29] J. L. Cardy ed., *Finite-Size Scaling*, North Holland, Amsterdam 1988.
- [30] N. Schultka and E. Manousakis, Phys. Rev. B **52**, 7528 (1995).
- [31] T. Schneider, R. Khasanov, K. Conder, and H Keller, J. Phys. Condens. Matter **15**, L763 (2003).
- [32] T. Schneider, Journal of Superconductivity, **17**, 41 (2004).
- [33] T. Schneider and D. Di Castro, Phys. Rev. B **69**, 024502 (2004).
- [34] C. Dasgupta and B. I. Halperin, Phys. Rev. Lett. **47**, 1556 (1981).